Proceedings of the 7th International Conference on HydroScience and Engineering

Philadelphia, USA September 10-13, 2006 (ICHE 2006)

ISBN: 0977447405

NUMERICAL SIMULATION OF COHESIVE AND NON-COHESIVE SEDIMENT ACCUMULATION IN TOKYO BAY

Thamnoon Rasmeemasmuang[1] and Jun Sasaki[2]

ABSTRACT

The characteristics of sediment accumulation in Tokyo Bay are simulated by a multi-class sediment model in which the sediment particles are classified based on the cohesive characteristics and particle sizes. The model linking hydrodynamics, wind-induced wave and bed shear stress modules can account for sediment transport, settling, deposition and resuspension processes. Simulation results show the high correlation between the sediment accumulation and the local bed shear stresses. The erosion of accumulated sediment in shallow waters is influenced mainly by the strong winds, whereas that in deep waters is influenced mainly by the strong currents. Availability of information of classified sediment components dedicates the detailed simulation in various aspects, e.g., the simulation of cohesive sediment content in accumulated sediments and muddy-sandy level of bed materials. Simulation of current bed characteristics shows the disappearance of sandy bed compared with the field investigation in the past. One of the causes of this phenomenon might be due to the decrease in shallow waters of the elevation of the sandy bed as a result of coastal-zone development projects.

1. INTRODUCTION

Tokyo Bay (see Figure 1.) is a semi-enclosed estuary, located in the central part of Japan and is well known as one of the most polluted and eutrophic embayment in Japan. It is approximately 50 km in length and 20 km in width, with an average of depth about 15 m. More than 90 percent of its coastline was reclaimed for the purposes of urban development and disaster prevention during the past five decades. This topographical characteristics has an effect upon that the residual current plays an important role in the sediment transport in the bay. The accumulation of sediments consequently brings about the significant effects on water quality and ecosystems because the accumulated sediments could intensify eutrophication through the release of nutrients after decomposition of the organic matter. In addition, the nutrient release from the sea bottom will affect the long-term nutrient cycling in the bay. This phenomenon of the organic-fertile sediments potentially increases the local sediment oxygen demand and develops hypoxia in the bottom water, that results in the mortality of benthic animals. In order to consider the strategy for the water quality

[1] Graduate Student, Department of Civil Engineering, Yokohama National University, Yokohama 240-8501, Japan (d04sc195@ynu.ac.jp)
[2] Associate Professor, Department of Civil Engineering, Yokohama National University, Yokohama 240-8501, Japan (jsasaki@cvg.ynu.ac.jp)

improvement in enclosed seas, it is necessary to understand the mechanism of the formation of the spatial distribution and the properties of accumulated bed materials.

A number of field investigations on sediment accumulation and bed characteristics in Tokyo Bay have been conducted. The bed characteristics of the whole part of Tokyo Bay were investigated before 1959 by Secretariat of Committee on Development in Tokyo Metropolitan Area. Matsumoto (1983) carried out an investigation on the spatial variation of the rate of mud accumulation in the whole part of Tokyo Bay based on the age presumption of the sediment cores by the lead 210 method. Gomyo et al. (1990) clarified the depositional characteristics of bottom sediment in the bay by in-situ observation. Sasaki and Igarashi (2005) investigated the spatial distribution of mud layer thickness at the head of Tokyo Bay based on acoustic sounding. At the present moment, analysis by numerical simulation is, however, still limited.

Development of sediment accumulation model is required to predict the large-scale and long-term accumulation of bed sediments. In most of the existing numerical researches with regard to suspended and accumulated sediments in bay scale, a representative class of sediment was applied that it is not able to give the essential details, for example muddy-sandy level or cohesive sediment content in accumulated bed sediments.

In this study, a multi-class sediment model for the scale of Tokyo bay was designed considering the balance of complexity in sediment processes. Sediments were classified into certain categories according to cohesive-predominant features and representative particle sizes. The present model was developed through the integration of the advection-diffusion transportation and settling process in water body together with deposition and resuspension at the interface between water body and sea bed for multi-class suspended particulate matter. The model was then applied to study the characteristics of accumulated sediments in the bay. Basic concept of modeling, computational results and discussion are presented in this paper.

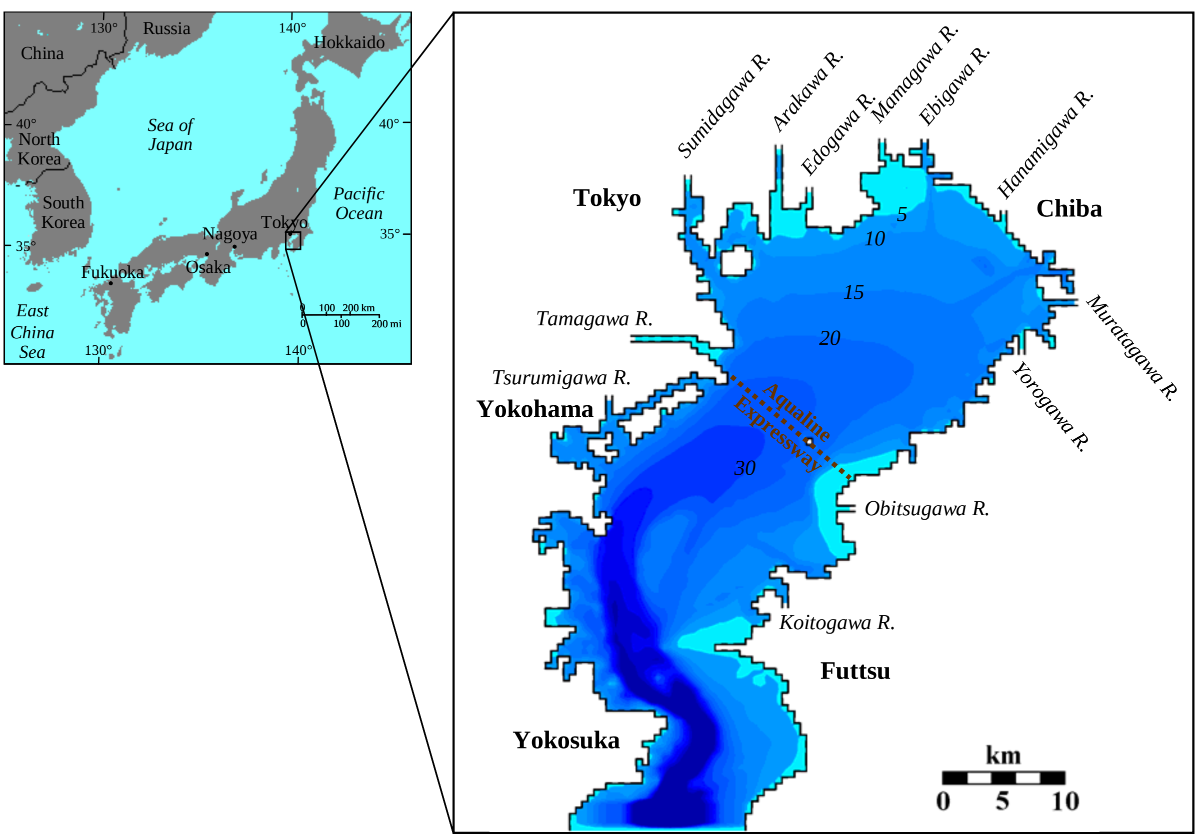

Figure 1 Location and Bathymetric Map of Tokyo Bay (depth in meter).

2. NUMERICAL MODELING

The numerical model consists of four main modules that are hydrodynamic model, wave hindcasting model, bed shear stress model and sediment model as shown in Figure 2.

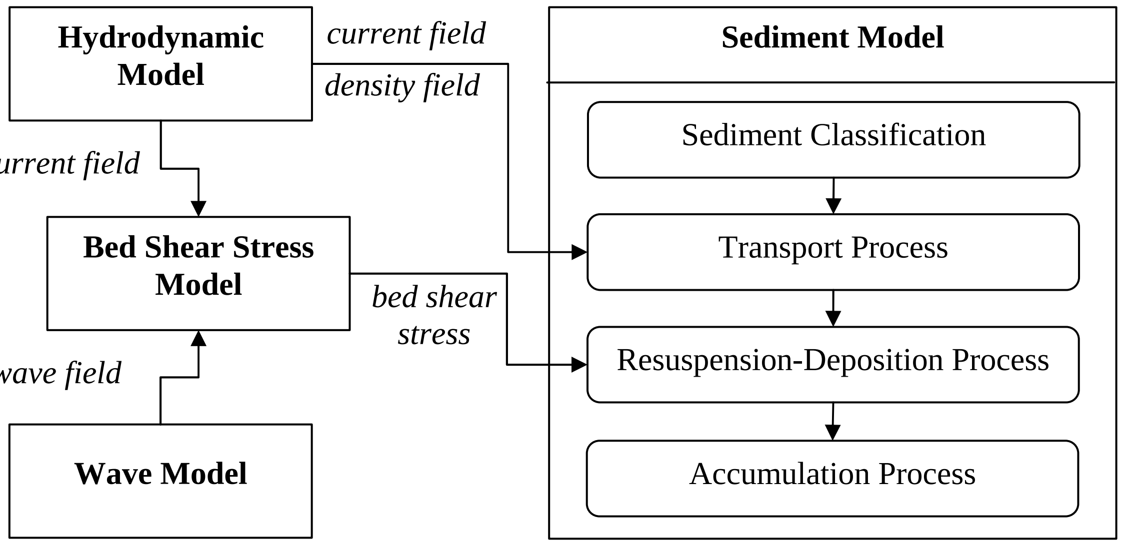

Figure 2 Numerical model framework

2.1 Hydrodynamic Model

Hydrodynamic model is required to simulate the current that is the most important driving force in sediment transport. This current field is also employed in order to obtain current-induced bed shear stress. Regarding computation for current fields, we adopted a quasi-three dimensional coastal circulation model developed by Sasaki et al. (1997; 1999). The model is a primitive equation model with hydrostatic and Boussinesq approximations in sigma coordinates. The governing equations, which are momentum equations for x and y directions and continuity equation, are given as follows:

$$\frac{\partial(Du)}{\partial t}+\frac{\partial(Duu)}{\partial x}+\frac{\partial(Dvu)}{\partial y}+\frac{\partial(D\dot{\sigma}u)}{\partial \sigma}=Dfv-\frac{gD}{\rho}\left[(\rho_0+\rho'\sigma)\frac{\partial\zeta}{\partial x}+\rho'(\sigma-1)\frac{\partial h}{\partial x}+\frac{\partial}{\partial x}\left\{D\int_{\sigma}^{-1}\rho' d\sigma\right\}\right]$$
$$+\frac{1}{D}\frac{\partial}{\partial\sigma}\left(A_v\frac{\partial u}{\partial\sigma}\right)+DA_h\left(\frac{\partial^2 u}{\partial x^2}+\frac{\partial^2 u}{\partial y^2}\right) \tag{1}$$

$$\frac{\partial(Dv)}{\partial t}+\frac{\partial(Duv)}{\partial x}+\frac{\partial(Dvv)}{\partial y}+\frac{\partial(D\dot{\sigma}v)}{\partial \sigma}=-Dfu-\frac{gD}{\rho}\left[(\rho_0+\rho'\sigma)\frac{\partial\zeta}{\partial y}+\rho'(\sigma-1)\frac{\partial h}{\partial y}+\frac{\partial}{\partial y}\left\{D\int_{\sigma}^{1}\rho' d\sigma\right\}\right]$$
$$+\frac{1}{D}\frac{\partial}{\partial\sigma}\left(A_v\frac{\partial v}{\partial\sigma}\right)+DA_h\left(\frac{\partial^2 v}{\partial x^2}+\frac{\partial^2 v}{\partial y^2}\right) \tag{2}$$

$$\frac{\partial\zeta}{\partial t}+\frac{\partial(Du)}{\partial x}+\frac{\partial(Dv)}{\partial y}+\frac{\partial(D\dot{\sigma})}{\partial\sigma}=0 \tag{3}$$

where t is time, x and y are the horizontal Cartesian coordinates, z is the vertical Cartesian coordinates upward from the still water level, u,v,w are the corresponding velocity components in the x, y and z directions, respectively, h and ζ are the water surface elevation from the still water level and the surface displacement respectively, the total depth $D = h + \zeta$, ρ is the density of seawater consisting of the reference density ρ_0 and the fluctuation ρ', f is the Coriolis parameter, g is the acceleration of gravity, A_h and A_v are the horizontal and vertical eddy viscosities, respectively, σ is a sigma-coordinate defined by $\sigma = (z+h)/D$, and $\dot{\sigma}$ is pseudo vertical velocity in σ coordinates and expressed by:

$$\dot{\sigma} = \frac{\partial \sigma}{\partial t} + u\frac{\partial \sigma}{\partial x} + v\frac{\partial \sigma}{\partial y} + w\frac{\partial \sigma}{\partial z} = \frac{\sigma}{D}\frac{\partial \zeta}{\partial t} + \frac{u}{D}\left(\frac{\partial h}{\partial x} - \sigma\frac{\partial D}{\partial x}\right) + \left(\frac{\partial h}{\partial y} - \sigma\frac{\partial D}{\partial y}\right) - \frac{w}{D}. \tag{4}$$

The transport equation for a scalar quantity ϕ in σ coordinates can be written as:

$$\frac{\partial(D\phi)}{\partial t} + \frac{\partial(Du\phi)}{\partial x} + \frac{\partial(Dv\phi)}{\partial y} + \frac{\partial(D\dot{\sigma}\phi)}{\partial \sigma} = \frac{1}{D^2}\frac{\partial}{\partial \sigma}\left(K_v \frac{\partial(D\phi)}{\partial \sigma}\right) + DK_h\left(\frac{\partial^2 \phi}{\partial x^2} + \frac{\partial^2 \phi}{\partial y^2}\right) + \psi(\phi) \tag{5}$$

where K_h and K_v are the horizontal and vertical kinematic eddy diffusivities, $\psi(\phi)$ is a source term. This transport equation is used for computation of temperature T and salinity S.

A semi-implicit finite difference approach was adopted to solve the equations, in which vertical advection and diffusion terms as well as the surface elevation related to surface gravity waves were discretized in implicit to enhance the model performance with respect to computation efficiency and robustness. The comparison between numerical results and the field data of the time variation of temperature and salinity was satisfactory (Sasaki and Isobe, 1999). Density field, which is a function of temperature and salinity, is consequently computed by the equation of state for seawater.

2.2 Wave Model

The wave model adopted is that of the United States Army Corps of Engineers (1994), which consists of two expressions; deep water formula and shallow water formula. Significant wave height and period, which are applied to calculate bed shear stress due to wave, are determined by equations (6) and (7) for deep water and (8) and (9) for shallow water, respectively.

$$\frac{gH}{U_A{}^2} = 1.6\times 10^{-3}\left(\frac{gF}{U_A{}^2}\right)^{\frac{1}{2}} \tag{6}$$

$$\frac{gT}{U_A{}^2} = 2.857\times 10^{-1}\left(\frac{gF}{U_A{}^2}\right)^{\frac{1}{3}} \tag{7}$$

$$\frac{gH}{U_A{}^2} = 0.283\tanh\left[0.530\left(\frac{gD}{U_A{}^2}\right)^{\frac{3}{4}}\cdot\tanh\left\{\frac{0.00565\left(\frac{gF}{U_A{}^2}\right)^{\frac{1}{2}}}{\tanh\left[0.530\left(\frac{gD}{U_A{}^2}\right)^{\frac{3}{4}}\right]}\right\}\right] \tag{8}$$

$$\frac{gT}{U_A} = 7.54\tanh\left[0.833\left(\frac{gD}{U_A{}^2}\right)^{\frac{3}{8}} \cdot \tanh\left\{\frac{0.0379\left(\frac{gF}{U_A{}^2}\right)^{\frac{1}{3}}}{\tanh\left[0.833\left(\frac{gD}{U_A{}^2}\right)^{\frac{3}{8}}\right]}\right\}\right] \tag{9}$$

where, H and T are significant wave height (m) and period (s) respectively, U_A is wind speed (m/s), F is the fetch (m) at the location in question, and D is the total depth (m).

2.3 Bed Shear Stress Model

In the sediment model described in the next sub-section, the deposition and resuspension processes of bed material are dependent on the combined wave-current bed shear stress τ_b which is divided into the wave-induced component τ_{bw} and the current-induced component τ_{bc}. We adopted the form of each stress as in equation (10) for current component and as in equation (11) for wave component as follows:

$$\tau_{bc} = \frac{\rho(u_b{}^2 + v_b{}^2)}{C_h{}^2} \tag{10}$$

$$\tau_{bw} = \frac{1}{2}\rho\, f_w \left|\hat{U}_b\right|^2 \tag{11}$$

where u_b and v_b are the current velocities for x and y directions on the bed, C_h is the bed stress coefficient for the current component, f_w is the bed stress coefficient for the wave component, and $\hat{U}_b$ is the amplitude of the wave induced oscillatory velocity and determined by:

$$\hat{U}_b = \frac{\pi H}{T\sinh(2\pi h / L)} \tag{12}$$

where L is the wave length obtained through the dispersion relationship.

2.4 Sediment Model

To simulate the bed characteristics, for instance, muddy-sandy level or cohesive sediment content in accumulated bed sediments, one representative category of sediment is not enough. We, thus, proposed a multi-class sediment model (Rasmeemasmuang and Sasaki, 2006) as a tool for this objective.

2.4.1. Classification of Sediments

The prominent aspect of cohesive behavior and the particle size were adopted as classification factors of sediments flowing from the river into the bay. In the present study, we classified the sediments into 4 categories; fine sand, coarse silt, fine silt, and clay particles. Fine sand and coarse silt particles are assumed that the non-cohesive characteristic is dominant, whereas fine silt and clay particles are assumed that the cohesive characteristic is dominant. The representative sizes of the particles of sediment were set by using the Krumbein phi scale, devised by Krumbein (1934), at the boundary between particles. Phi scale, representative size and percentage in suspended sediments in river water are summarized in Table 1.

Table 1 Sediment classification in the present model

Parameter	Fine sand	Coarse silt	Fine silt	Clay
Phi scale	4	5	6	8
Representative diameter (μm)	62.5	31.3	15.6	3.9
Percentage in suspended sediments in river water	5	20	50	25

2.4.2. Transport Process

Transport process of all of the sediments is governed by the advection-diffusion equation where the vertical advection includes the settling velocity of particles. The equation in sigma coordinates can be written as:

$$\frac{\partial(DC)}{\partial t}+\frac{\partial(uDC)}{\partial x}+\frac{\partial(vDC)}{\partial y}+\frac{\partial\left((\dot{\sigma}+\dot{\sigma}_s)DC\right)}{\partial\sigma}=DK_h\left(\frac{\partial^2 C}{\partial x^2}+\frac{\partial^2 C}{\partial y^2}\right)+\frac{1}{D}\frac{\partial}{\partial\sigma}\left(K_v\frac{\partial C}{\partial\sigma}\right) \quad (13)$$

where C is the sediment concentration of each particle and $\dot{\sigma}_s$ is the settling velocity in sigma coordinates estimated as w_s / D where w_s is the settling velocity in Cartesian coordinates.

In estuaries and coastal waters, the settling velocity of fine-grained cohesive particles is significantly different from those of coarse-grained non-cohesive particles. Cohesive particles will collide with each other and form flocs, called flocculation process dependent on which sediment concentration. For non-cohesive particles, individual-particle settling velocity can be adopted, which is determined from the balance of gravitational and drag forces (Stokes' Law) as in equation (14). For cohesive sediments, we adopted the standard expression of concentration-dependant settling velocity as in equation (15):

$$w_s=\frac{1}{18}\frac{gd^2(\rho_p-\rho)}{\eta} \quad \text{, for non-cohesive particles} \quad (14)$$

$$w_s=\alpha C^m \quad \text{, for cohesive particles} \quad (15)$$

where d is the particle diameter, ρ_p is the density of the particles, ρ is the density of the fluid, η is the molecular viscosity of the medium, α is a coefficient dependent on the mineralogy of the particles and m is an empirical parameter typically ranging from 1 to 2 (e.g., Mehta, 1986; van Leussen, 1994). After tuning the parameters with the data of Thorn (1981), Ross (1988) and Wolanski et al. (1992), α of 0.005 and m of 1.4 were used in this study.

At the surface boundary, zero flux of materials was applied, whereas at the bottom boundary, material flux was defined as either resuspension or deposition flux expressed by:

$$K_v \frac{\partial C}{\partial \sigma} = D \cdot (F_R - F_D) \tag{16}$$

where F_R and F_D are fluxes of resuspension and deposition respectively, described in the following sub-section.

2.4.3. Resuspension and Deposition Processes

At the interface of water body and sea bed, a model was established using critical bed stress formulas (Krone-Partheniades formulas from Odd and Murphy, 1992) to represent the deposition and resuspension processes. The fluxes of deposited and resuspended matter are:

$$F_D = \begin{cases} w_s C\left(1 - \dfrac{\tau_b}{\tau_d}\right), & \text{for } \tau_b < \tau_d \\ 0\,, & \text{for } \tau_b \geq \tau_d \end{cases} \tag{17}$$

$$F_R = \begin{cases} E_0\left(\dfrac{\tau_b}{\tau_e} - 1\right), & \text{for } \tau_b > \tau_e \\ 0\,, & \text{for } \tau_b \leq \tau_e \end{cases} \tag{18}$$

where E_0 is an empirical erosion rate constant typically ranging from 0.002 to 0.02 $gm^{-2}s^{-1}$ (e.g., Kappe et al., 1989; Winterwerp, 1989), τ_d and τ_e are the critical bed shear stresses for deposition and resuspension, respectively.

The values of critical bed shear stress both for deposition and for resuspension are dependent on the classes of sediments because the coarser-grained sediments resuspend more difficult and deposit easier than the finer-grain sediments do. In the model, the critical bed shear stresses for deposition and for resuspension are given in Table 2.

Table 2 Critical bed shear stress parameters used in the present model

Parameter	Fine sand	Coarse silt	Fine silt	Clay
Critical bed shear stress for deposition (N/m^2)	0.25	0.20	0.10	0.05
Critical bed shear stress for resuspension (N/m^2)	0.25	0.20	0.15	0.10

2.4.4. Accumulation Process

Flux of resuspension F_R and flux of deposition F_D through the interface of water body and sea bed must affect temporal change in the mass of accumulated bed sediments, which can be expressed by:

$$\frac{\partial B}{\partial t} = F_D - F_R \tag{19}$$

where B is the material accumulation in mass per unit area.

3. OUTLINE OF SIMULATION

The model was forced by winds, air temperatures, relative humidity, short wave radiations and precipitations recorded hourly by Chiba Meteorological Observatory, Japan Meteorological Agency. Tides at the open boundary were taken from the Tide Table of Japan Meteorological Agency. River discharges were taken from the daily discharge data of Ministry of Land, Infrastructure and Transport for Tamagawa River and Edogawa River. Discharges for the other rivers were set to be proportional to the discharge of Edogawa River with multiplying magnification factor determined by comparing annual mean discharges. The suspended sediment concentrations in water of 12 main rivers discharging into Tokyo Bay were obtained from the monthly data of National Institute of Environment Studies.

Numerical simulation was performed for one year period throughout 1996 to obtain integrated results of sediment accumulation all over the bay. To obtain realistic initial conditions of accumulated sediments, we executed a preliminary run in 1995 and then applied the final results to the initial conditions for the computation in 1996. The computational domain was divided by 500 m times 500 m horizontal grid, with 10 vertical sigma levels. Computation time increment was set to be 150 seconds based on the condition for numerical stability.

4. RESULTS AND DISCUSSIONS

4.1 Time Series of Sediment Accumulation

The present model is capable of simulating time series of accumulated sediment entirely in Tokyo Bay as shown in Figure 3 where outputs were made every 30 days throughout the year of 1996. The simulation shows that sediments discharging from river mouths gradually deposit on the bed in the vicinity of river mouths, such as the vicinity of the mouths of Sumidagawa, Arakawa, Edogawa and Tamagawa Rivers. After time marching, the sedimentation inside the middle part of bay is seen likewise. Sediment accumulation in the region of bay mouth might be caused by the resuspended sediments from the bottom of the neighborhood of the bay mouth. This resuspension is influenced by the tremendous bed shear stress around that area. The relationship between the pattern of sediment accumulation and bed shear stress is elucidated in more details in Section 4.3.

The rate of sediment accumulation varied in time and space. Mostly the variation of the accumulation rate was gentle, apart from the time interval between 180th day and 240th day as shown in Figure 3f, 3g and 3h in which the rate of accumulation around the head of the bay was very high. The erosion process can, furthermore, be found in some places on occasions. Investigation on the factors influencing on the sediment accumulation and inducing the aforementioned phenomena was conducted and explained in the following part.

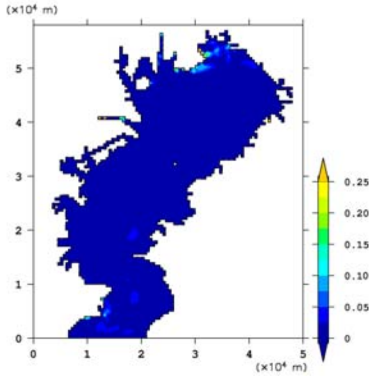

a) 30 days lapsed

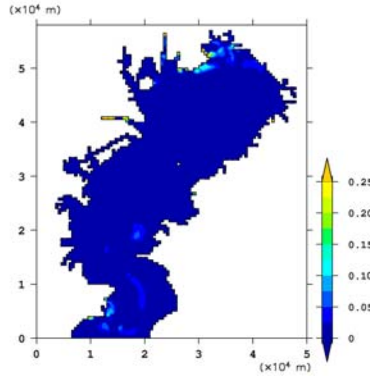

b) 60 days lapsed

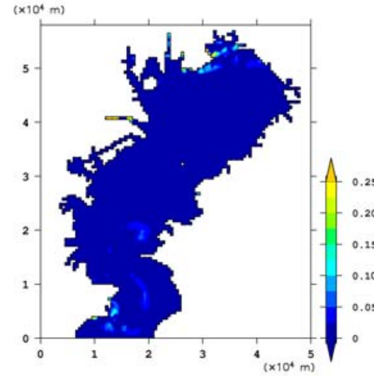

c) 90 days lapsed

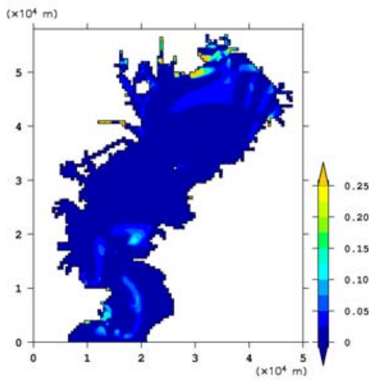

d) 120 days lapsed

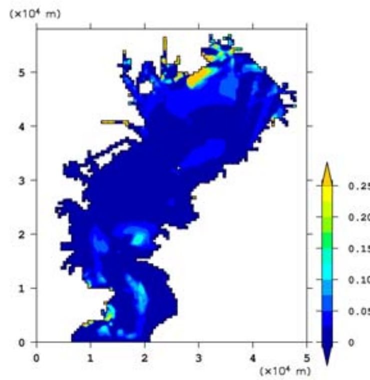

e) 150 days lapsed

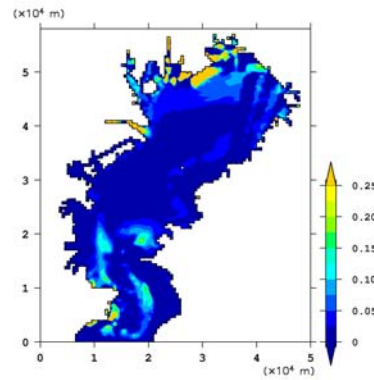

f) 180 days lapsed

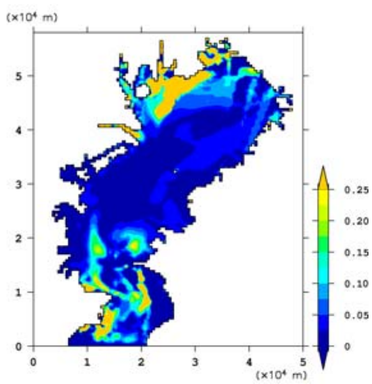

g) 210 days lapsed

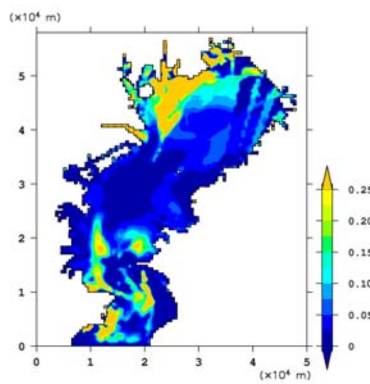

h) 240 days lapsed

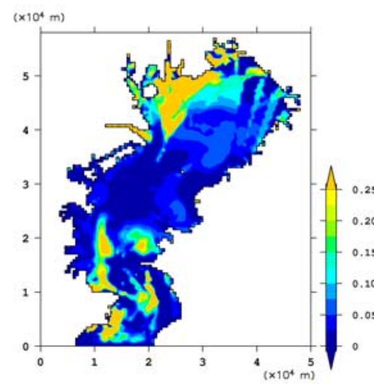

i) 270 days lapsed

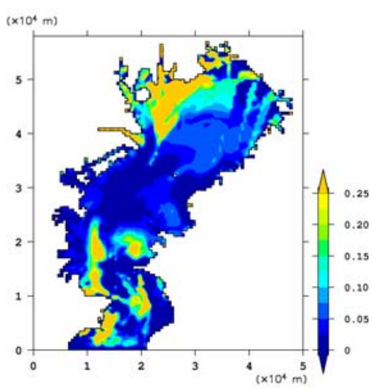

j) 300 days lapsed

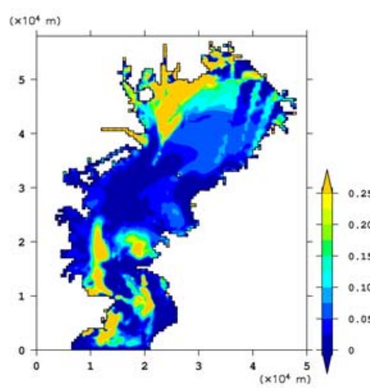

k) 330 days lapsed

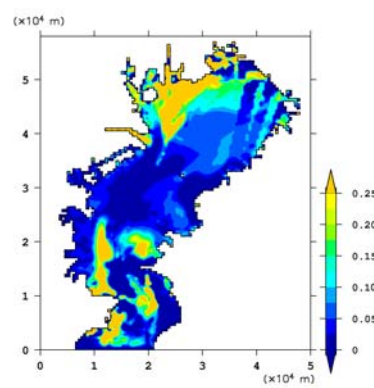

l) 360 days lapsed

Figure 3 Simulation results of sediment accumulation (g/cm^2) every 30 days.

4.2 Effects of Meteorological and Hydrodynamic Factors on Sediment Accumulation

To analyze the effects of meteorological and hydrodynamic factors on the sediment accumulation, the computational results at representative study points were collected every three days throughout one year, and compared with meteorological and hydrodynamic data. The first one of the study points is in shallow water in front of Edogawa River with 2.0 m of depth and the other is in deeper water in the central part of the head of the bay with 17.3 m of depth (see Figure 4).

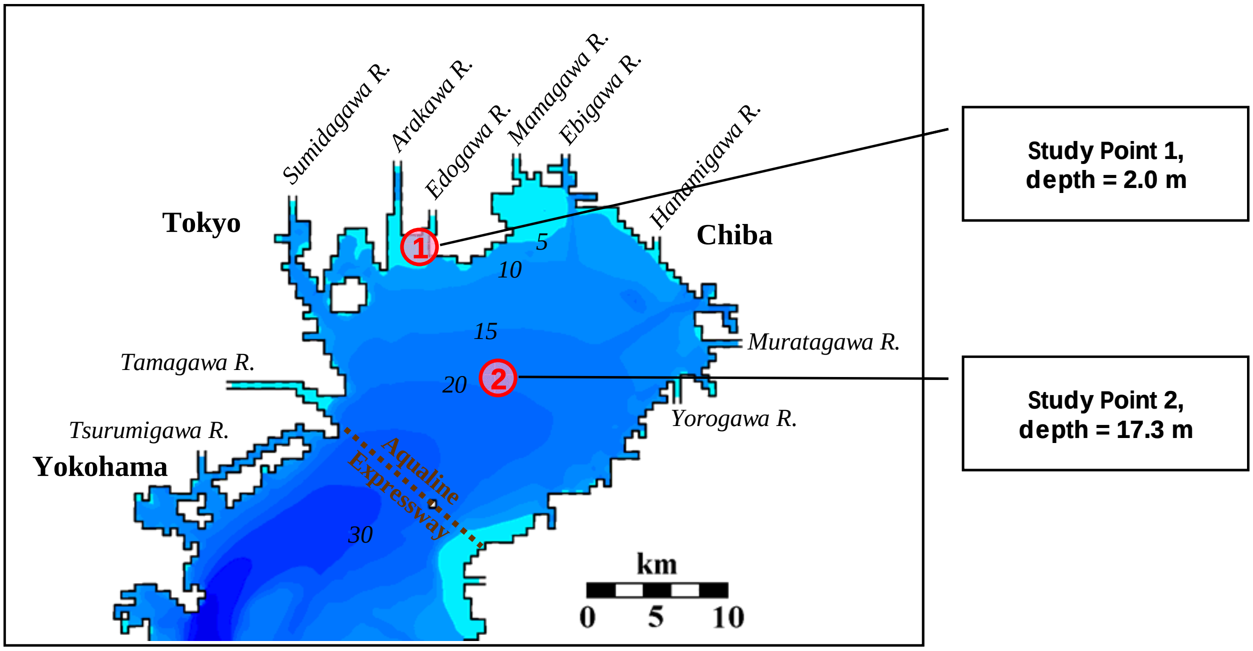

Figure 4 Location of numerical study points.

Figure 5 shows the comparison of time series of wind data, wave-induced bed shear stress at study point 1, sediment discharge from Edogawa River and sediment accumulation at study point 1. During the periods under southwest-ward strong wind conditions, the winds cause high waves in the vicinity of shallow water and then high waves thrust the strong wave-induced bed shear stresses. The strong bed shear stresses consequently cause the resusupension of bed sediments or the erosion of accumulated bed sediment.

Moreover, the comparison shows that the amount of sediment discharge from Edogawa River directly effects the sediment accumulation at the study point 1 with small time lag. The condition of extreme sediment discharge from the major rivers along the coast at the head of the bay, e.g., Edogawa, Arakawa and Sumidagawa Rivers, occasionally causes the high rate of accumulation around the bay head.

Figure 6 presents the comparison of time variation in horizontal current speed, current-induced bed shear stress and sediment accumulation at study point 2. The temporal change of sediment accumulation at study point 2 in deeper water is smoother than that at study point 1 in shallower water. The strong currents straightforwardly cause the high current-induced bed shear stresses that accordingly lead to the erosion of accumulated bed sediment.

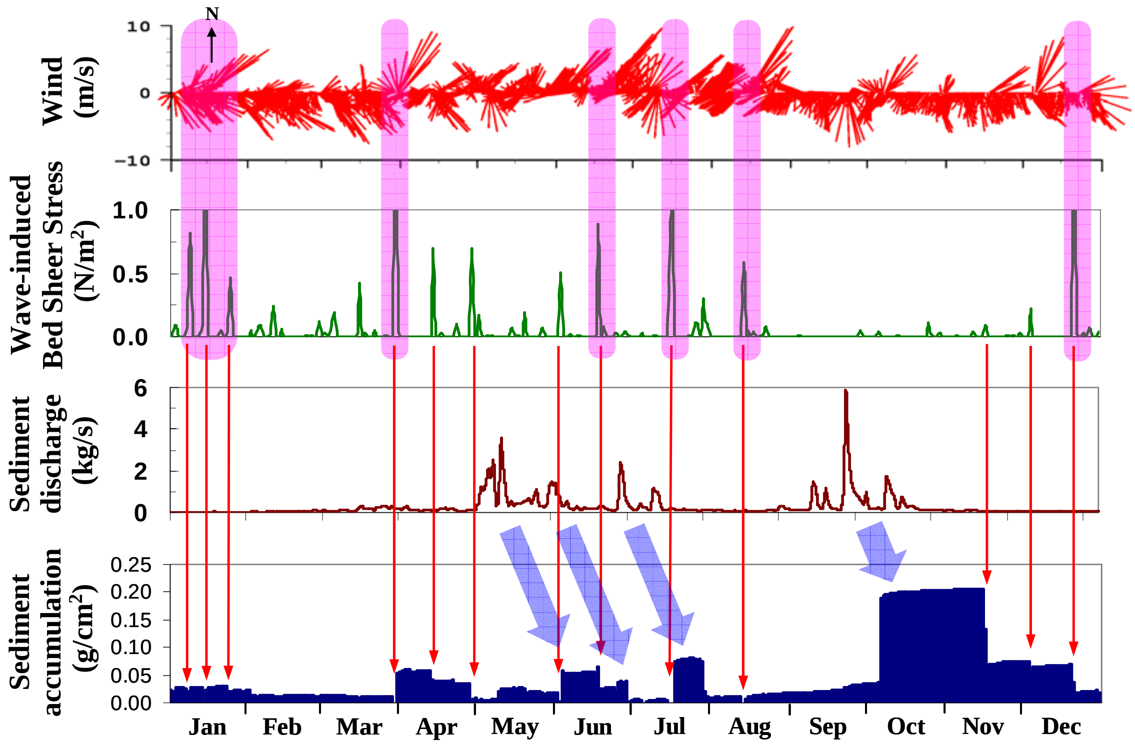

Figure 5 Comparison of time-varying wind vector, wave-induced bed shear stress at study point 1 (the origin of each wind vector is on the x-axis), sediment discharge from Edogawa River and sediment accumulation at study point 1.

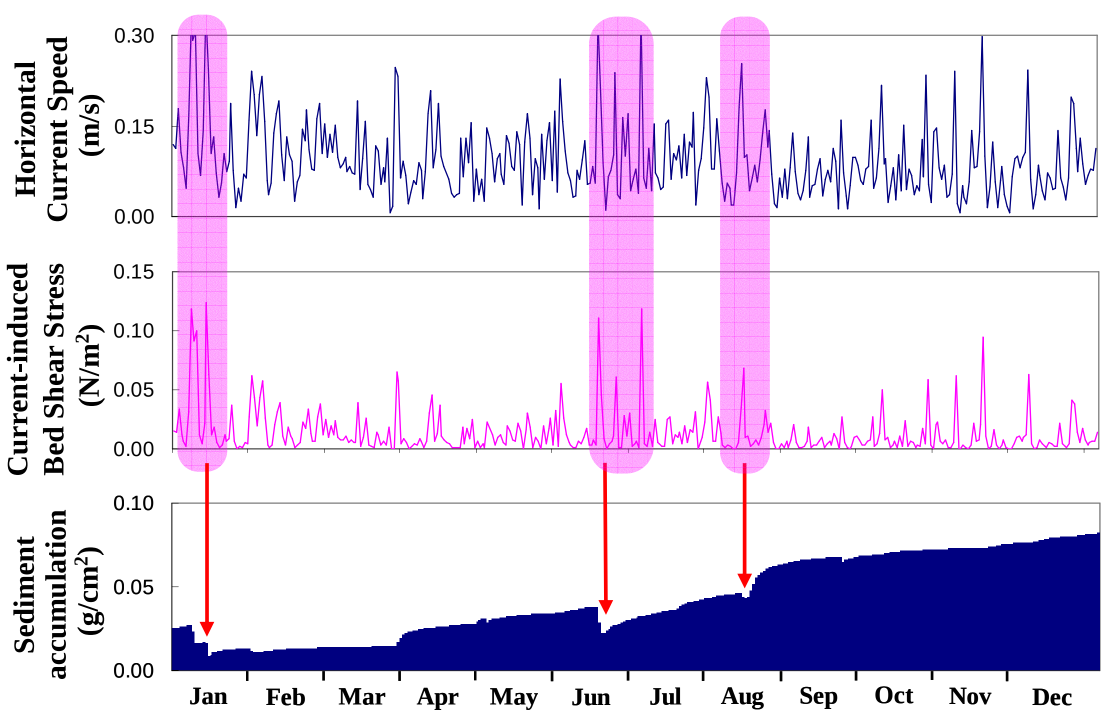

Figure 6 Comparison of time-varying horizontal current speed, current-induced bed shear stress and sediment accumulation at study point 2.

4.3 Pattern of Sediment Accumulation

The pattern of sediment accumulation in whole of Tokyo Bay was explained reasonably by Rasmeemasmuang and Sasaki (2006) that higher rate of accumulation occurs in the vicinity of major river mouths and the rate decreases with increasing distance from the mouths. This description is also consistent with field investigations Matsumoto (1983) as well as Sasaki and Igarashi (2005).

Less accumulation was, nevertheless, found in some regions even near the river mouths. The relationship between total accumulation and average bed shear stress obtained from bed shear stress model throughout the year of 1996 is shown in Figure 7. In several regions near the river mouths, less accumulation or erosion occurs because of high wave-induced bed shear stress in shallow water, for instance, around the sea bed in front of Mamagawa River and Ebigawa River as well as around the end of Aqualine Expressway in front of Obitsugawa River, encircled by solid line in Figure 7a and 7b.

A lower rate of accumulation was, moreover, found around the bay mouth shown by dashed line in Figure 7a and 7c. This phenomenon occurs as a result of strong current-induced bed stress in the vicinity of bay mouth.

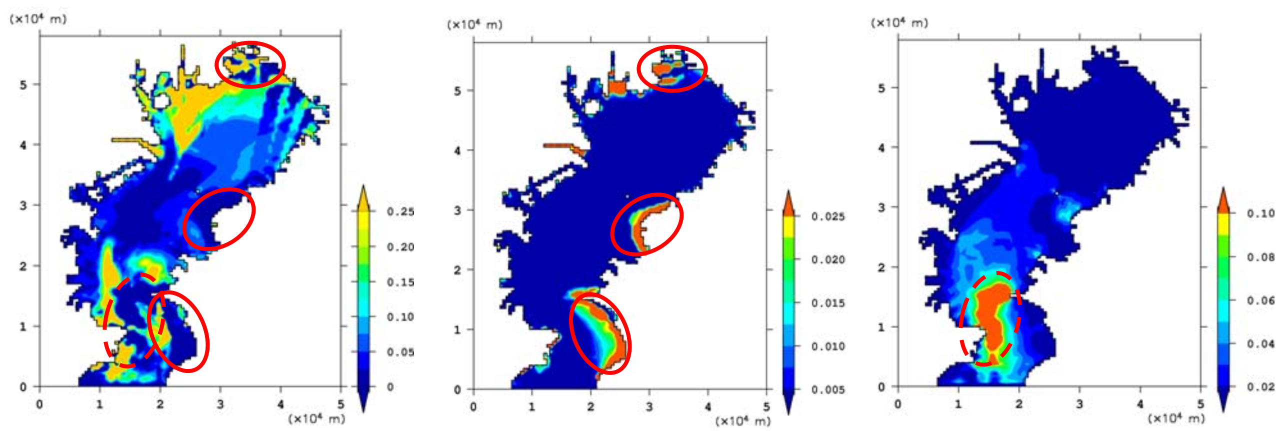

a) b) c)

Figure 7 a) Total sediment accumulation, b) Average wave-induced bed shear stress (N/m^2) and c) Average current-induced bed shear stress (N/m^2), computed throughout the year of 1996.

4.4 Sediment Accumulation of Each Classified Material

The privilege of the multi-class sediment model is that the information of sediment accumulation for each component is yielded (Rasmeemasmuang and Sasaki, 2006). Sediment accumulation for fine sand, coarse silt, fine silt and clay components are shown in Figure 8a to 8d, respectively.

Coarse-grained particles, fine sand and coarse silt, mostly settle down in the vicinity of river mouths after flowing into the bay because of their larger settling velocities, while fine-grained particles, fine silt and clay, can transported farther by currents and fall down even the places farther from river mouths.

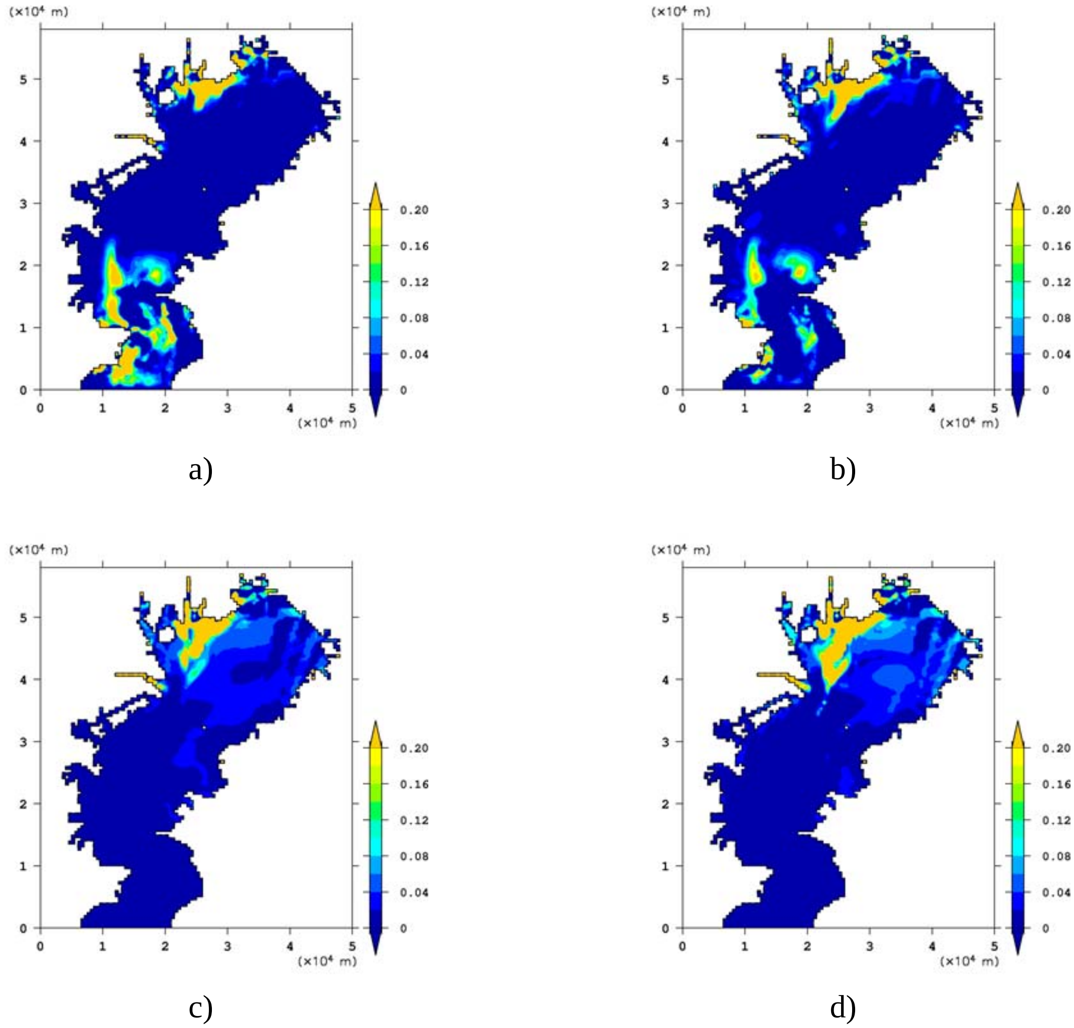

Figure 8 Sediment accumulation for each component (g/cm^2): a) fine sand component, b) coarse silt component, c) fine silt component and d) clay component.

4.5 Simulation of Cohesive Sediment Content in Accumulated Sediments

From the concept of particle classification that fine sand and coarse silt are defined as non-cohesive sediment whereas fine silt and clay are defined as cohesive sediment, we computed the cohesive sediment content in total accumulated sediment as shown in Figure 9. Simulation result displays high cohesive sediment content in the central part of the inner bay. From the bay head to the middle, the cohesive content is mostly over 50%; meanwhile it is very low in the vicinity of the bay mouth where the fine-grained cohesive sediment cannot settle down because of strong current around the mouth.

This simulation is a pilot study of sediment quality modeling in semi-enclosed coastal waters. In the next step, the delicate classification of suspended particulate matters, for example, taking organic matters into account, will be performed so as to model and analyze the quality of accumulated sediments.

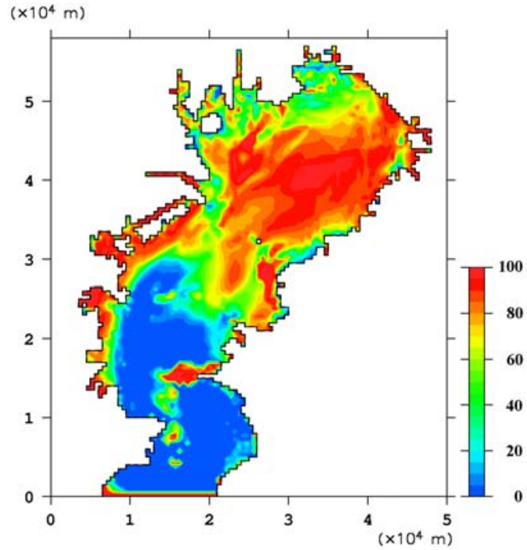

Figure 9 Percentage of cohesive sediment content in accumulated sediments.

4.6 Simulation of Bed Characteristics

To simulate the muddy-sandy characteristics of bed materials, we classified silt and clay particles as 'mud' and then calculate the percentage of mud content in accumulated sediment which now comprises mud and fine sand fractions. If accumulated sediment contains more than 90% of mud, we defined it as 'mud'; 50% to 90% of mud as 'sandy mud', 10% to 50% of mud as 'muddy sand' and less than 10% mud as 'fine sand'. Moreover, in case that any area contains very small amount of accumulated sediment, 0.001 g/cm^2 used in this simulation, we assumed in that area sediment cannot deposit because of high bed shear stress and only coarse-grained sediment, i.e. 'rock' or 'coarse sand', exist.

Figure 10a shows the field investigation of bed characteristics before 1959 by Secretariat of Committee on Development in Tokyo Metropolitan Area (cited from Kaizuka, 1993) and Figure 10b shows the computed bed characteristics in 1996. Although the overall patterns of the by-1959 investigated and the 1996 simulated bed characteristics are roughly resemble, i.e., the feature of muddy bed distribution in the central part of the bay or the coarse-grained-material bed around the bay mouth, the differences in details of both bed characteristics are obviously seen. The characteristics of bed materials have considerably changed during three decades, particularly in the inner part where the area of sandy bed from simulation in 1996 extremely decreased or nearly vanished, compared with the past bed characteristics. This simulation of bed characteristics is in good agreement with the field investigation of Sasaki and Igarashi (2005) reporting that in inner part of Tokyo Bay, the sea bed was covered by averagely 10 cm to 50 cm of soft mud layer.

One of the causes of the disappearance of sandy bed in the inner Tokyo Bay might be the change of coastal topography. The comparison of the investigated and simulated bed characteristics is shown once again in Figure 11 to clearly observe the coastal zone changes in the inner part of the bay. During these decades, the rapid growth of economics and urban development in Japan has been driving the coastal zone development. Several ports and an airport together with vertical seawalls which protect the cities against coastal disasters have been continuously constructed along the coastline of the inner Tokyo Bay. The land reclamations caused the loss of shallow water areas and brought about the stagnant waters in which bed shear stress is averagely rather small. In this kind of stagnant waters, the fine-grained sediments preferably settle down and accumulate with the small rate of resuspension process.

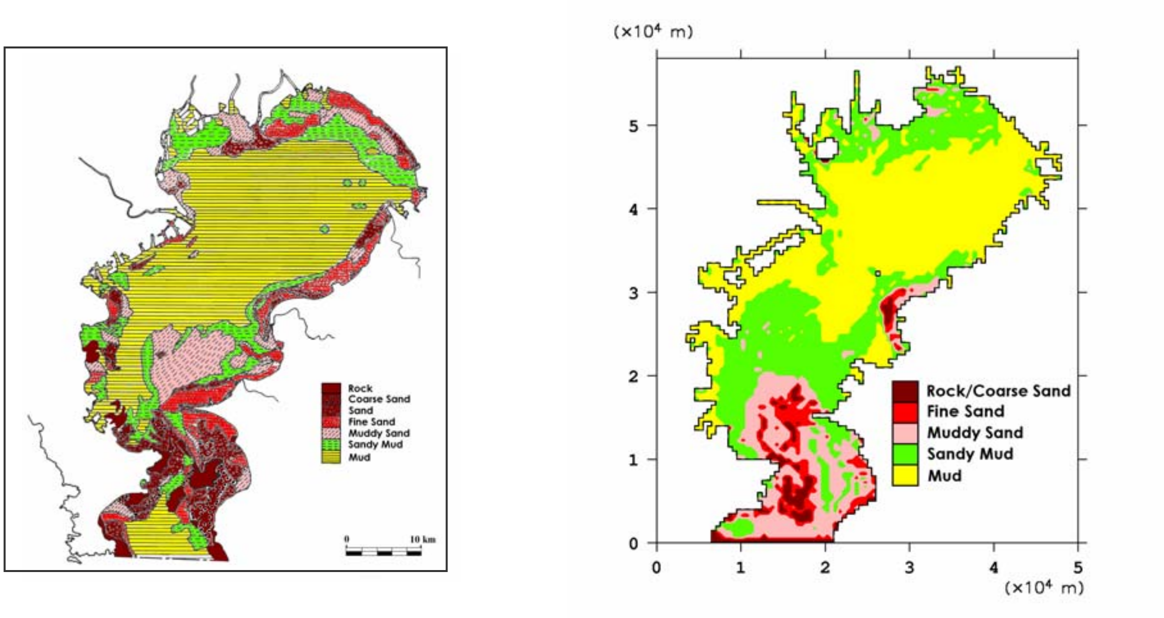

a) b)

Figure 10 a) The investigated bed characteristics before 1959 (after Kaizuka, 1993). b) The simulated bed characteristics in 1996.

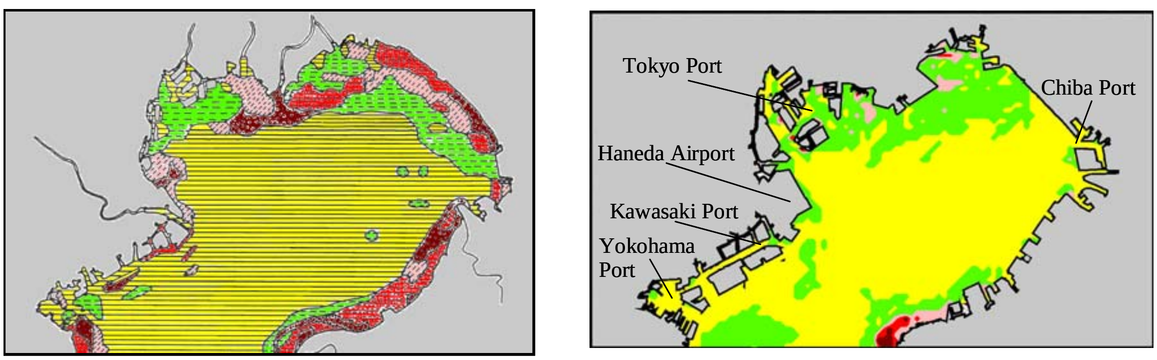

Figure 11 Comparison of the bed characteristics investigated before 1959 and the simulated bed characteristics in 1996 in inner Tokyo Bay.

5. CONCLUSIONS

The present paper presents the simulation of sediment accumulation in the whole of Tokyo by a multi-class sediment model, integrated with hydrodynamics and wave modules. The model can account for transportation, settling, deposition and resuspension processes of sediments. Concept of particle classification by cohesive characteristics and particle sizes is adopted. Numerical studies show that the temporal and spatial characteristics of sediment accumulation are considerably related to metrological and hydrodynamic features, in particular the local bed shear stress. Time variation of sediment accumulation in shallow waters is more dynamic than that in deep waters. The erosion of accumulated sediments in shallow waters is caused mainly by the strong winds in direction that induces high waves, whereas in deep waters it is caused mainly by the strong currents.

Muddy-sandy characteristic of bed materials is simulated and compared with the filed investigation in the past. The numerical results successfully reproduce the overall pattern of the sediment properties in the field except the nearshore zones at the head of the bay where the disappearance of the sandy beds is visible. This discrepancy is caused by the loss of the tidal flats and shallows due to the reclamation of the foreshore. The computational results also give us the fine structures of sediment grain size distribution. This kind of information is very useful for the modeling of the distribution of organic matter in the bottom sediments since its concentration in the sediments is highly correlated with the content of the fine particles through the adsorption process.

The present model will be further extedned to include the transport of organic material together with an ecosystem model to reproduce the detailed sediment quality and the interaction between the pelagic and bed regimes.

ACKNOWLEDGEMENTS

This present work was partially funded by the JSPS Grant-in-Aid for Scientific Research (B) No.15360263. The authors would like to thank National Institute of Environment Studies for public-used data. The first author gratefully acknowledged the financial support of Ministry of Education, Culture, Sports, Science and Technology for his study in Yokohama National University.

REFERENCES

Gomyo, M., Yauchi, E. and Otsuki, T. (1990). “Properties of mud sediment in Tokyo Bay”, Proc. Coastal Eng., JSCE, 37, pp. 848-852. (in Japanese)

Kaizuka, S. (1993). Topography, Geology and Water Quality in Tokyo Bay, Tsukiji-Shokan, Japan. (in Japanese)

Kappe, B.P., van Koningsbruggen, P. and Voogt, L. (1989). “Erosion of silt resulting from navigation”, Integrated Water Management Ketelmeer, Rijkswaterstaat RIZA, Lelystad.

Krumbein, W. C. (1934). “Size frequency distribution of sediments”, J. Sediment Petrol, 4, pp. 65-77.

Matsumoto, E. (1983). “The sedimentation environment of Tokyo Bay”, Chikyukagaku (Geochemistry), pp. 27-32. (in Japanese)

Mehta, A.J. (1986). “Characteristics of cohesive sediment properties and transport processes in estuaries,” Estuarine Cohesive Sediment Dynamics, In: Mehta, A.J.(Ed), Lecture Notes on coastal and Estuarine Studies 14 Springer, pp. 290-325.

Odd, N.V.M. and Murphy, D.G. (1992). “Particulate pollutants in North Sea”, Report SR 292, Hydraulics Research, Wallingford.

Rasmeemasmuang, T. and Sasaki, J. (2006). “Numerical analysis of characteristics of annual accumulated sediment in Tokyo Bay”, Proc. of TECHNO-OCEAN 2006 / 19th JASNAOE Ocean Engineering Symposium, paper number 31, 8 pages.

Ross, M.A. (1988). “Vertical structure of estuarine fine sediment suspension”, PhD thesis, Coastal and Oceanographic Engineering Department, University of Florida.

Sasaki, J. and Igarashi, M. (2005). “Spatial characteristics of soft-mud accumulation in inner part of Tokyo Bay, Japan”, Proc. of 3rd Int. Conf. on Asian and Pacific Coast, pp. 564-580.

Sasaki, J. and Isobe, M. (1999). “Development of a long-term predictive model of water quality in Tokyo Bay”, Proc. of 6th Conf. on Estaurine and Coastal Modeling, ASCE, pp. 564-580.

Sasaki, J., Isobe, M., Watanabe, A. and Gomyo, M. (1997). “Numerical study on ‘Aoshio’, upwelling of anoxic water, in Tokyo Bay”, Proc. of 27th Congress of IAHR, B, pp. 641-646.

Thorn, M.F.C. (1981). "Physical processes of siltation in tidal channels", Proc. Hydraulic modeling applied to marine engineering problems, ICE, London, pp. 47-55.

United States Army Corps of Engineers (1994). Shore Protection Manual.

van Leussen, W. (1994). "Estuarine macroflocs and their role in fine-grained sediment transport", PhD Thesis, University of Utrecht.

Winterwerp, J.C. (1989). "Flow-induced erosion of cohesive beds; a literature study", Delft Hydraulics Report No. 25.

Wolanski, E., Gibbs, R.J., Mazda, Y., Mehta, A.J. and King, B. (1992). "The role of turbulence in settling of mudflocs", Journal of Coastal Research, 8 (1), pp. 35-46.